9-2009

A study on the effect of random placement and orientation on the resonance of multiple split ring resonators

Michael Buscher
University of Arkansas, Fayetteville

A Study on the Effect of Random Placement and Orientation on the Resonance of Multiple Split Ring Resonators

---

University of Arkansas
College of Engineering
Department of Electrical Engineering
Honors Thesis Report

Student: Michael Brandon Buscher
Faculty Advisor: Dr. Vasundara Varadan

Abstract

This thesis project experimentally studies the effect of placing split-ring oscillators (SRR) in a non-periodic arrangement with random orientation. This is contrary to typical structures which are simulated as a single unit cell with a periodic boundary condition to emulate an infinite array of SRR's. Samples are measured using a near-field free-space measurement system with full Thru, Reflect, Line (TRL) calibration and the application of time domain gating. Results, in the form of scattering (S) parameters, are compared with previous measurements of periodic SRR structures in order to study the influence, if any, of periodicity in the frequency response of a metamaterial sample. Experimental results show that the spatial organization of SRR's have no significant effect on the resonance of the structure.

Table of Contents

List of Figures

1.0 Introduction

1.1 Background

The objective of this experiment is to examine the effect of placing Multiple Split Ring Resonators (SRR's) in a non-periodic arrangement. Typically, it is convenient for both design and simulation to create samples composed of a 2-dimensional periodic lattice of SRR structures. This arrangement allows for simulation to be simplified to a unit cell with a periodic boundary condition imposed on the borders of the cell. An as of yet unstudied aspect of the split ring resonator is the effect of a layout which places SRR's in a non-periodic arrangement.

1.2 Scope of Project

This experiment will examine, through measurement of Scattering (S) parameters, the effect, if any, of a non-periodic arrangement of SRR structures in two orientations as compared with corresponding periodic arrangements of SRR. Firstly, a planar sample in which the vector normal to the surface of the sample is parallel with the incident wave, and secondly, a sample composed of strips in which the normal vector is perpendicular to the incident beam. The measurements will be performed for both un-backed and metal-backed cases in each configuration.

2.0 Theoretical Background

2.1 Microwave Measurement

This research utilized a near field scanning system, shown in Figure 1, designed and implemented by the faculty research advisor, Dr. Vasundara Varadan. The HVS Free Space Measurement System is capable of performing near-field microwave measurements from the C band through the W band, 4.8 – 110 GHz, and is fully automated. This automation, two linear and two rotary degrees of freedom per antenna provides a precise system with a high degree of repeatability for microwave measurements.

The system makes use of two focused beam antennas with Gaussian intensity and a constant phase front in the measurement plane. Due to these properties, the Gaussian beam may be assumed to be analogous to plane wave illumination within the -3 dB beam width, equal to one wavelength of the beam in free space.

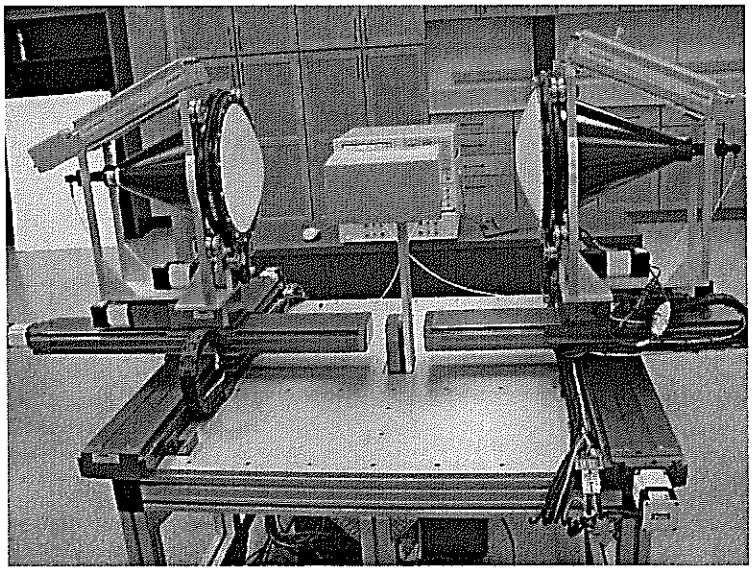

Figure 1 – HVS Automated Free Space Measurement System. The system is fully automated and is capable of measurements from 4.8 – 110 GHz. The sample being measured is placed between the antennas on the vertical positioner axis, in place of the box.

2.1.1 Measurement Calibration

Samples are measured after performing full Thru, Reflect, Line (TRL) calibration. This calibration technique defines the reference planes of measurement for ports 1 and 2 to be exactly on the surfaces of the sample being measured. The calibration process is performed as follows.

- **Reflection standard measurement.** A polished metal plate, as close to a perfect electric conductor as possible, is used to reflect all signal back to the transmit (Port 1) antenna.
- **Line standard measurement.** With nothing between the transmit (Port 1) antenna and the receive (Port 2) antenna, a separation of $\frac{\lambda_0}{4}$, where λ_0 is the mid-band wavelength.
- **Thru standard measurement.** For the Thru measurement, the two focal planes are set with no separation.

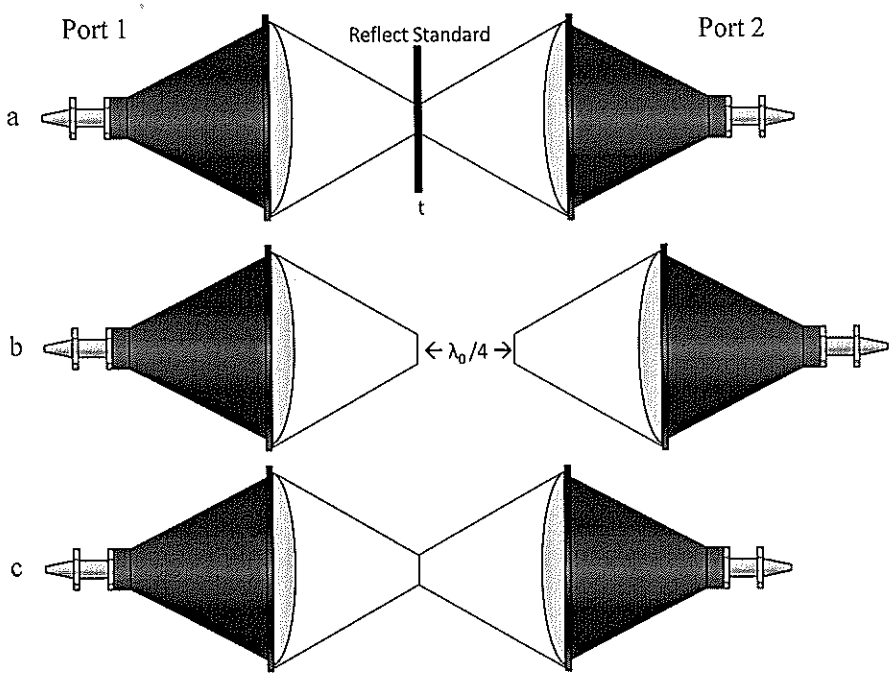

Figure 2 – TRL calibration. (a) Reflect measurement, all signal should reflect directly back to Port 1 antenna; (b) Line measurement, signal passes through "line" composed of air; (c) Thru measurement, all signal from Port 1 is passed to Port 2 with no transmissi

2.1.2 Time Domain Gating

To further eliminate systematic errors caused by impedance mismatches at connectors, time domain gating is applied to the measured data. Time domain gating is performed by performing an inverse Fourier transform and smoothing any signal components that occur outside of the timeframe of the measurement. The signal is then brought back to the frequency domain through a Fourier transform.

2.2 Plasmonic Oscillator

Plasmonic oscillators are passive LC RF oscillators that operate by the excitation of plasmons on the surface metallization of the structure. These plasmons, which are essentially clumps of electrical charge, are excited by the resonant response of the structure and oscillate around the structure, effectively absorbing incident power. This response is observed as minima in the measured S parameter data.

2.3 Split Ring Resonator

Split Ring Resonators are a form of plasmonic oscillator. An SRR is composed of N concentric rings, each with a gap offset 180° from the other, but for the purpose of this experiment, N is fixed as 2. In addition to the material properties of the substrate on which the structure is printed, there are 5 basic design parameters which must be taken into consideration for the design of an SRR. These are the metallization thickness (t), line width (w), the spacing between traces (s), the width of the ring gap (g), and the length of the outermost ring (l). These parameters account for all dimensions needed to lay out an SRR. The necessary material properties are the relative permittivity of the substrate (ε_r), relative permeability of the substrate (μ_r) which is assumed to be 1 as the substrate is non-magnetic, and the substrate thickness (h).

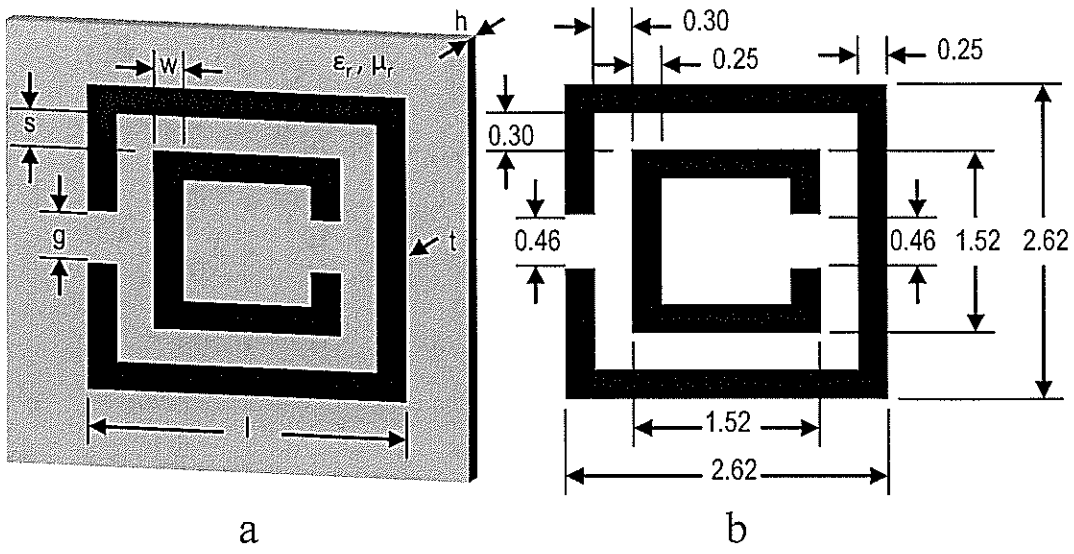

Figure 3 - SRR dimensions. (a) 4 dimensions needed for SRR design (l, g, s, w, t, h, ε_r, $\mu_r = 1$), (b) dimensions, in mm, of MOLIC SRR printed on an FR4 substrate of thickness 0.75 mm, $\mu_r = 1$, $\varepsilon_r = 4+j0.08$, metallization thickness of 17μm, and resonant frequency at 10.4 GHz[2]

2.3.1 Equivalent Circuit Modeling

Based on the assumption that a split ring resonator is in essence a simple LC oscillator, an equivalent circuit model is introduced to estimate the Plasmon frequency of the structure as seen in Figure 4. The quasistatic approximation derived by Bilotti, *et al* [1], provides the ability to roughly compute the resonant frequency of the SRR in the case of 2 or more rings given the physical dimensions of the structure. The lumped circuit elements of this model are derived from the capacitance between rings of the SRR and the inductance of the metalized rings of the SRR. Loss elements are introduced to take into account Ohmic dissipation in the conductor and the dielectric substrate on which the SRR is printed.

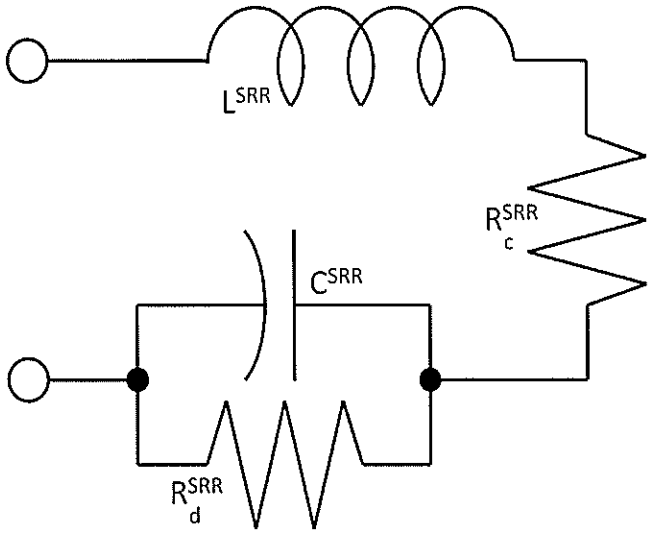

Figure 4 - Equivalent circuit model for split ring resonator structure with lumped elements representing the series inductance (L), series conductor loss (R_L), and shunt capacitance (C) and shunt dielectric loss (R_d)

The design equations presented by Bilotti, *et al.*,[1,3] are applied to compute the approximate resonant frequency for the case of a general SRR structure as follows:

- The SRR inductance is computed as a function of the average strip length over both rings and the fill ratio, ρ, which accounts for the amount of metal over the area of the SRR.

$$L^{MSRR} = \frac{\mu_0}{2}\frac{l_{avg}}{4}(4.86)\left[\ln\left(\frac{0.98}{\rho}\right) + 1.84\,\rho\right]$$

- The total SRR capacitance is calculated by factoring the per-unit-length capacitance for two parallel strips, C_0, for all rings in the structure. An important thing note about this equation is that the variable 'g' is not present. Though there is a gap in the ring, its effects are assumed to be negligible.

$$C^{MSRR} = \frac{N-1}{2}[2l - (2N-1)(w+s)]C_0$$

- The Ohmic dissipation for the SRR structure is taken by multiplying the per-unit-length resistance of the structure by the same loop the inductance was factored.

$$R_C^{MSRR} = \frac{\rho_c}{w\,t}\frac{L^{MSRR}}{\mu_0}$$

- Dielectric loss is computed through multiplying the dielectric resistance $\frac{1}{\sigma_d}$ by a function that decreases as N increases

$$R_d^{MSRR} = \frac{1}{\sigma_d}\frac{s}{h[l-(2w+s)]}\frac{l_{avg}}{4l}$$

- The average length of the SRR traces are computed using this geometric function

$$l_{avg} = 4[l-(N-1)(w+s)]$$

- The fill ratio is a function relating the amount of metal covering the SRR cell

$$\rho = \frac{(N-1)(w+s)}{l-(N-1)(w+s)}$$

- The capacitance per unit length between 2 strips of width 'w' and separation 's.' K(x) is defined to be the complete elliptical integral of the first kind.

$$C_0 = \varepsilon_0\varepsilon_r^{sub}(\varepsilon_r,h,w,s)\frac{K\left(\sqrt{1-k^2}\right)}{K(k)} \quad | \quad k = \frac{s}{s+2w}$$

- To compute the effective relative permittivity of the structure, determined heuristically is as follows:

$$\varepsilon_r^{sub}(\varepsilon_r,h,w,s) = 1+\frac{2}{\pi}\arctan\left[\frac{h}{2\pi(w+s)}\right](\varepsilon_r-1)$$

By restricting the value 'N' to $N = 2$, the design equations can be simplified to the following:

(1) $L^{SRR} = 2.43(l-w-s)\left[\ln\left(0.98\frac{l-w-s}{w+s}\right)+1.84\frac{w+s}{l-w-s}\right]$

(2) $C^{SRR} = \left[l-\frac{3}{2}(w+s)\right]C_0$

(3) $R_C^{SRR} = \frac{\rho_c}{w\,t}\left\{2.43(l-w-s)\left[\ln\left(0.98\frac{l-w-s}{w+s}\right)+1.84\frac{w+s}{l-w-s}\right]\right\}$

(4) $R_d^{SRR} = \frac{1}{\sigma_d}\left(\frac{l-w-s^2}{hl\,(l-2w-s)}\right)$

These equations are then used to approximately calculate the resonant frequency of a 2 ring SRR structure. Using the dimensions from Figure 3 as a reference, the following parameters are applied to equations 1 – 4.

$s = 0.3\ mm = 3 \times 10^{-4} m$ $\quad$ $h = 0.75\ mm = 7.5 \times 10^{-4}\ m$

$w = 0.25\ mm = 2.5 \times 10^{-4} m$ $\quad$ $\varepsilon_r = 4, \mu_r = 1$

$g = 0.46\ mm = 4.6 \times 10^{-4} m$ $\quad$ $t = 17\ \mu m = 1.7 \times 10^{-5} m$

$l = 2.62\ mm = 2.62 \times 10^{-3} m$

By applying these values, the following results are obtained:

$L^{SRR} = 11.3\ nH$ $\quad$ $R_c^{SRR} = 0.0361\ \Omega$

$C^{SRR} = 0.0347\ pF$ $\quad$ $R_d^{SRR} = 24.5\ k\Omega$

$$f_0 = \frac{1}{2\pi} \frac{1}{\sqrt{L^{SRR} C^{SRR}}} = 8.03\ GHz$$

2.3.2 Planar vs. Strip Samples

SRR samples are measured in one of two configurations, as shown in Figure 5, a sample composed of many strips or a planar sample. Both samples have beneficial qualities that make them worthy of studying. A strip sample will see excitation due to both the incident electric (E) field and the magnetic (H) field, causing a significantly stronger resonance than a planar sample. This benefit is given at the cost of practicality. While a planar sample will only be excited by the incident electric (E) field, it is far more practical for implementation as it is merely metallization on a single substrate. In order to measure samples in the strip configuration a sample holder is required to maintain strip spacing.

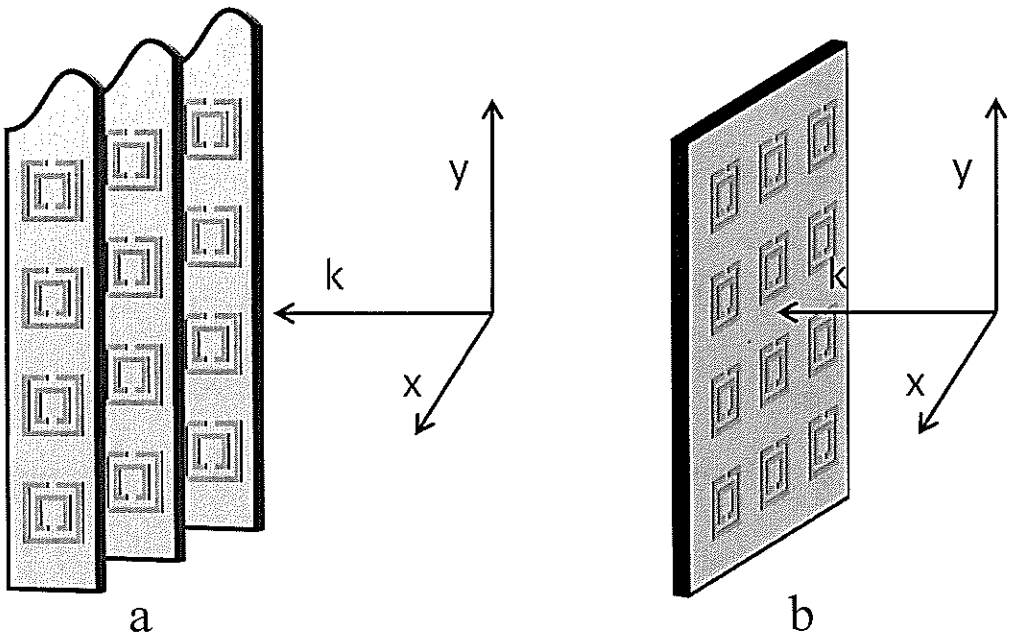

Figure 5 – Configurations of SRR sample. "k" represents the direction of wave propagation. (a) strip sample composed of many strips, and (b) a planar sample in which all SRR's are contained within the plane of the substrate surface. By changing the configuration of the sample, the resonance strength is affected.

2.3.3 Standard SRR Samples

The orientation of the gap in the rings of the SRR with respect to the polarization angle of the incident electromagnetic signal is crucial to obtaining a resonance response. There are 3 typical arrangements for SRR structures in a periodic lattice.

- SRR1 – Split ring resonator oriented such that the ring gap is perpendicular to the polarization of the incident electric (E) field. All SRR's are excited by incident plane wave.
- SRR2 – SRR's are placed in a periodic lattice with random orientation. This arrangement will theoretically allow SRR's to become excited for any arbitrary angle of polarization.
- SRR3 – SRR oriented with gap parallel to polarization of incident electric (E) field. No resonance is observed in this case.

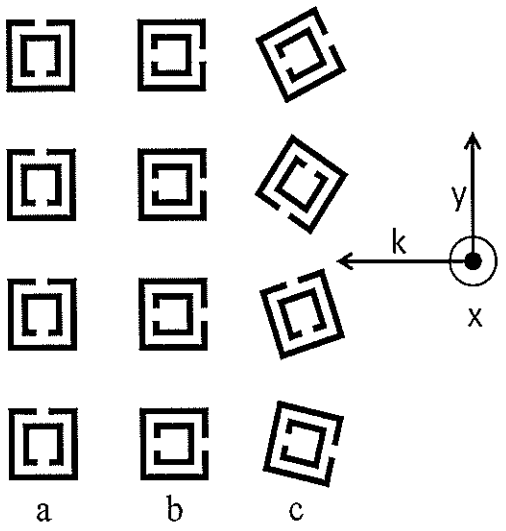

Figure 6 – Typical SRR arrangements; assume E-field is polarized in the y direction. (a) SRR1 with gap oriented perpendicular to the E-field polarization. (b) SRR3, gap is oriented parallel to E-field. (c) SRR2, resonators are oriented at random angles with respect to the incident E-field.

3.0 Sample Fabrication

3.1 Introduction

In addition to the samples already present at the Microwave and Optics Laboratory for Imaging and Characterization (MOLIC), several new samples were designed for the purpose of this experiment. These samples, a strip sample and a planar sample, both with random orientation and SRR placement, were designed and fabricated using copper metallization and an FR4 substrate.

3.2 SRR Structure Design

In order to effectively compare the results for a new sample configuration, it should be designed to exhibit the same response as preexisting samples. With this fact in mind, samples consisting of SRR's with the same dimensions are designed and implemented .

3.3 SRR_{Random} Sample Layout

In order to rapidly and efficiently place the split ring resonators, a program was written in Microsoft Visual Basic to compute the planar coordinates and angle of orientation for all components. An algorithm was run to ensure that there was no overlap when placing an SRR. This verification was performed by iterating over all existing SRR's and calculating the vector distance between the desired coordinate and the coordinates of the i^{th} SRR.

$$For\ all\ i\ \in [0, N_{SRRs\ Placed}],\ if\ \sqrt{(X_{SRR\ new} - X_{SRR\ i})^2 + (Y_{SRR\ new} - Y_{SRR\ i})^2}\ > (R_{new\ SRR} + RSRR\ i\ then\ Place\ SRR$$

A graphical representation of this check is shown in Figure 7, and source code for the program is presented in Appendix A.

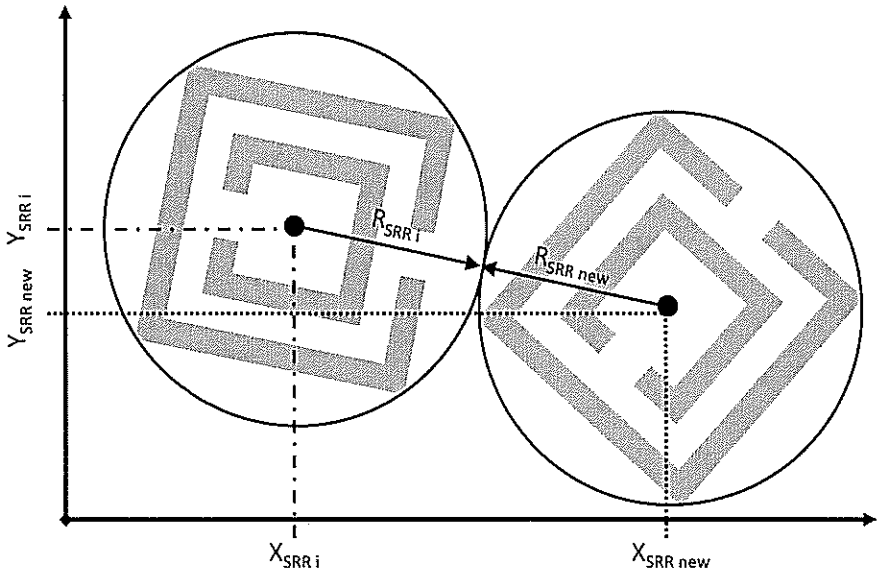

Figure 7 - Split Ring Resonator Placement. Circumscribing circles are used to calculate potential for overlap based on SRR coordinates. If the sum of the radii is greater than the displacement of the two SRR's then there is no overlap.

The program was run for samples consisting of 500 SRR's over an area of 15 cm x 15 cm, generating both strip and planar samples. After the desired coordinates were generated, they were manually supplied to a CAD package. The CAD drawings for all samples were then combined into a single file and exported to a Gerber file used to fabricate the samples.

4.0 Results

4.1 Introduction

Samples are measured over X band, 8.2 to 12.4 GHz, in order to observe the resonance in the frequency response for SRR structures designed to operate at 10.4 GHz. The sample configurations measured are as follows:

- Planar SRR samples without backing
- Planar SRR samples with metal backing
- SRR strip samples
- SRR strip samples with metal backing

4.2 Planar samples without backing

A planar SRR structure will exhibit a purely electrical resonance. The effect that this has is weaker resonance strength. There is no apparent frequency shift between the SRR_{random} sample and the other SRR structures. The SRR_{random} sample does exhibit a much weaker resonance than the other structures. This is due to a lower density of SRR's; the standard samples consist of 900 SRR's while the SRR_{random} sample consists of only 500 SRR's.

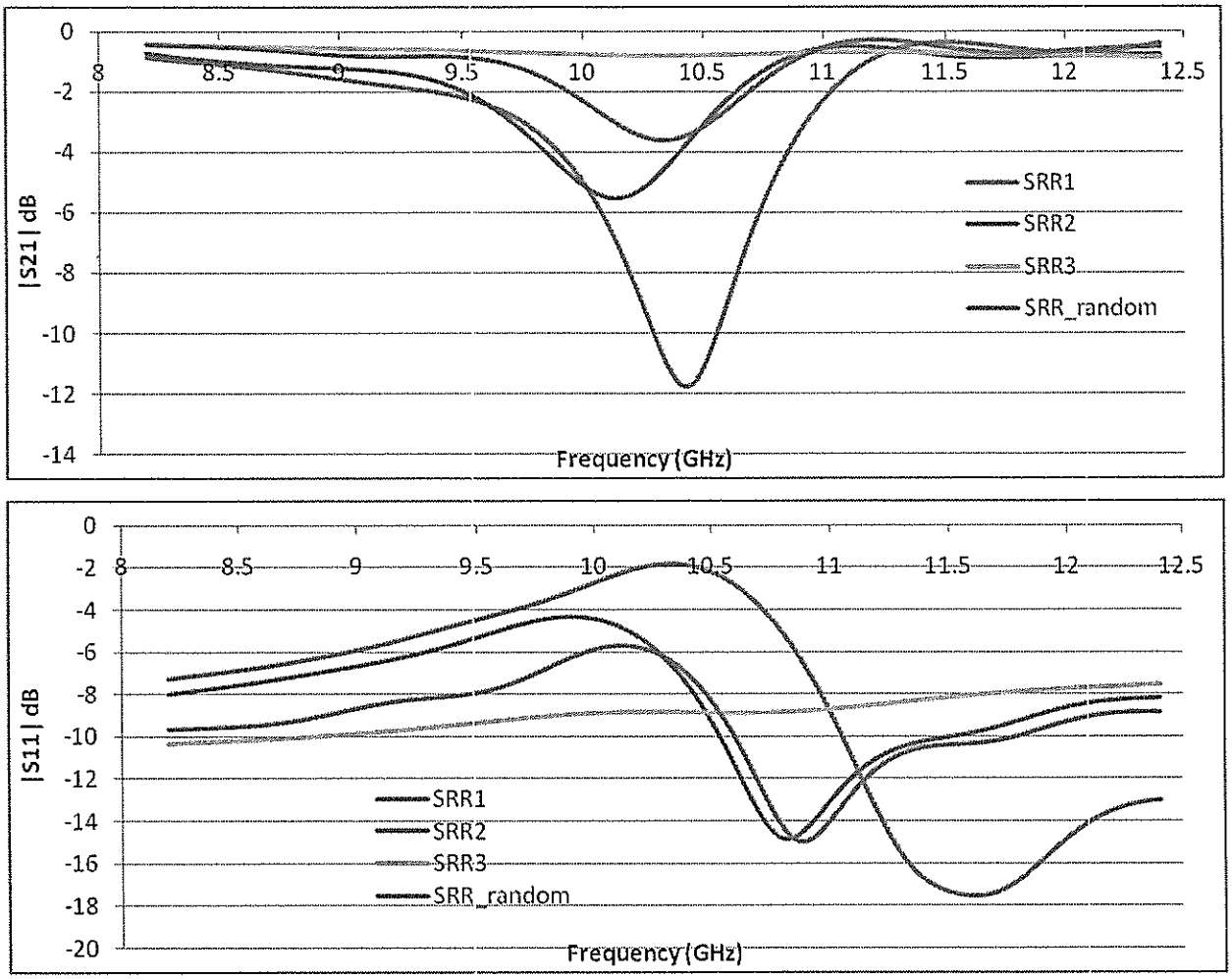

Figure 8 – Experimental data measured for planar SRR samples. Resonance occurs at 10.4 GHz for SRR1, SRR_{random}, and 10.1 GHz for SRR2. The random sample has a weaker resonance due to having fewer SRR's being present than in the other samples.

4.3 Planar samples with metal backing

When a metal plate is placed behind the sample, all incident power is reflected back through the sample instead of being allowed to pass on to the receive (port 2) antenna. This causes the S_{21} parameter to be extremely small, near the dynamic floor of the measurement equipment. The focus shifts from transmission minima to the reflection minima. Since the signal is reflected through the SRR structure a second time, a much stronger resonance is observed than for the un-backed case.

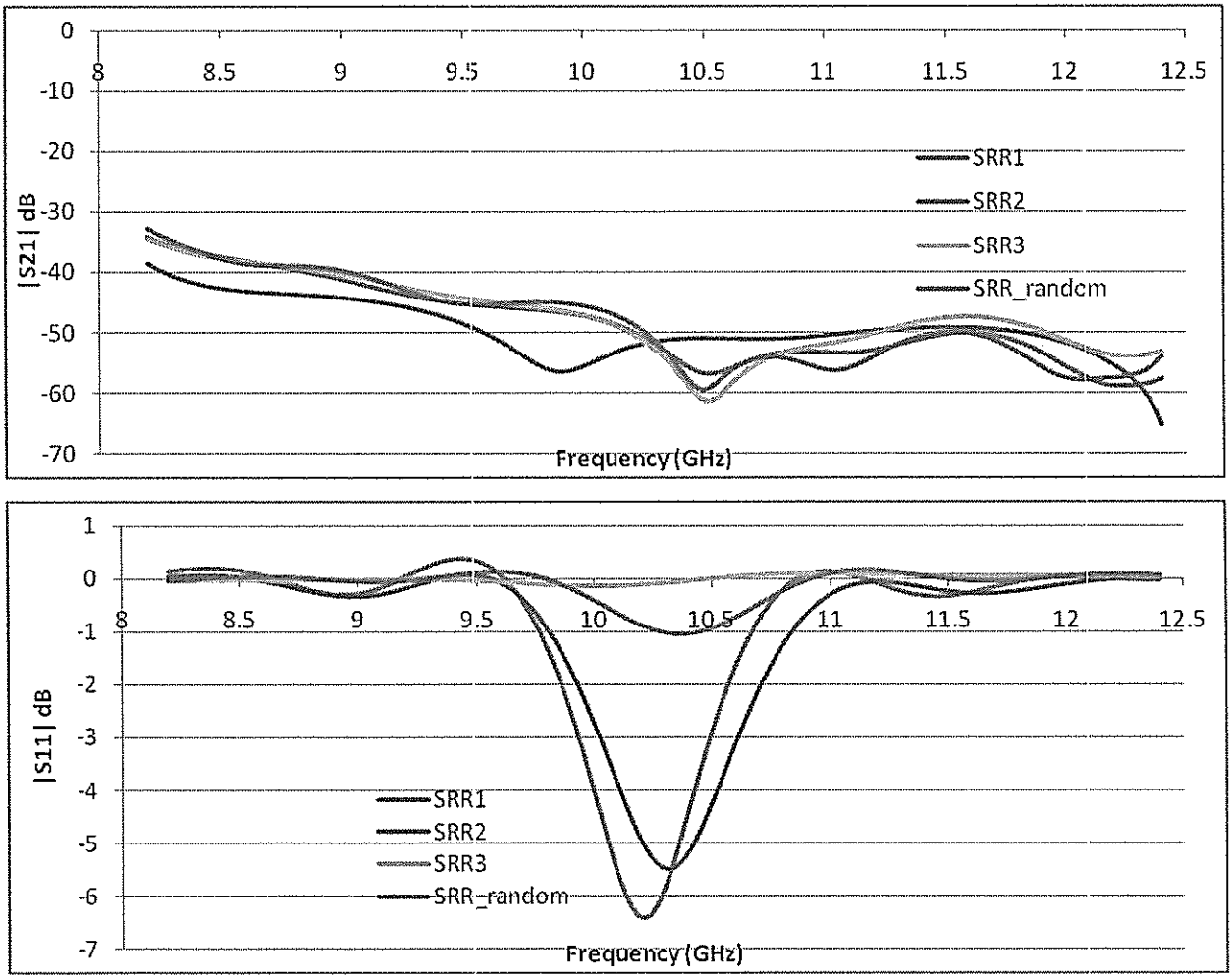

Figure 9 – Experimental data for planar samples with metal backing. $|S_{21}|$ near the dynamic floor of the network analyzer because the metal backing causes all incident power to be reflected back to the input port. Resonance is now observed in S_{11}, reflection.

4.4 Strip samples without backing

Strip samples have the added benefit of a magnetic resonance, greatly improving the depth of resonance. The reflection and transmission minima also occur at roughly the same frequency in this case. Though these characteristics are highly desirable, this material is far less practical than the planar version of the same properties because it is comprised of a series of strips suspended in air rather than a simple layer of metallization on the substrate material.

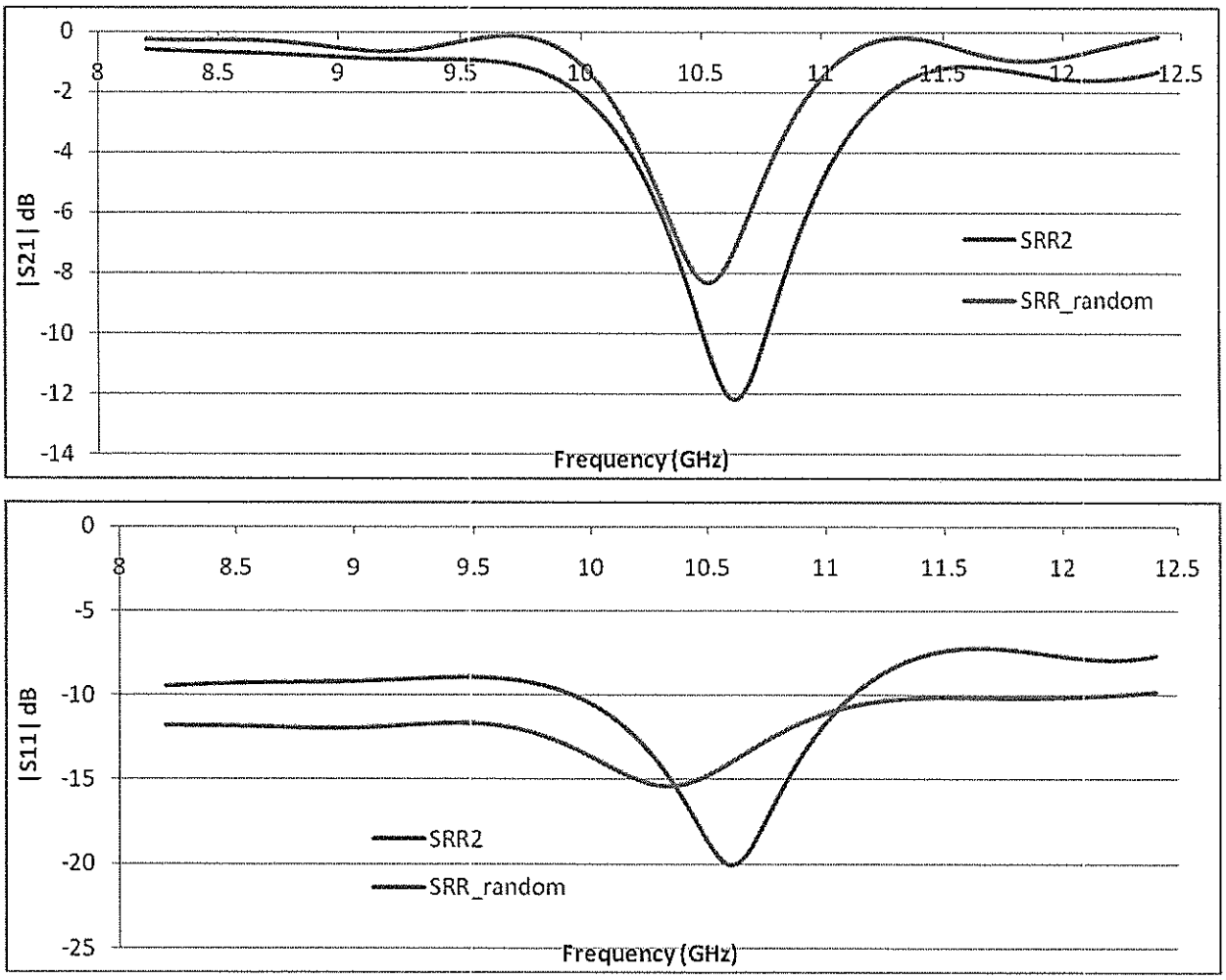

Figure 10 – Measured data for SRR strip samples without backing. The resonance is much stronger than for the planar case. The S_{11} minima and the S_{21} minima also occur at roughly the same frequency for a strip sample.

4.5 Strip samples with metal backing

Due to the fact that no signal is transmitted to port 2, only reflection data is reported for this configuration. With metal backing, the deepest resonance of all measured samples is observed. The S_{11} minima are -18 dB and -27 dB for SRR_{random} and SRR2 respectively. These resonances correlate with near 100% power absorption; all incident power is absorbed by the plasmonic resonance. It is also noted that the resonant frequency for SRR2 was shifted above the 10.4 GHz at which the sample was designed to operate.

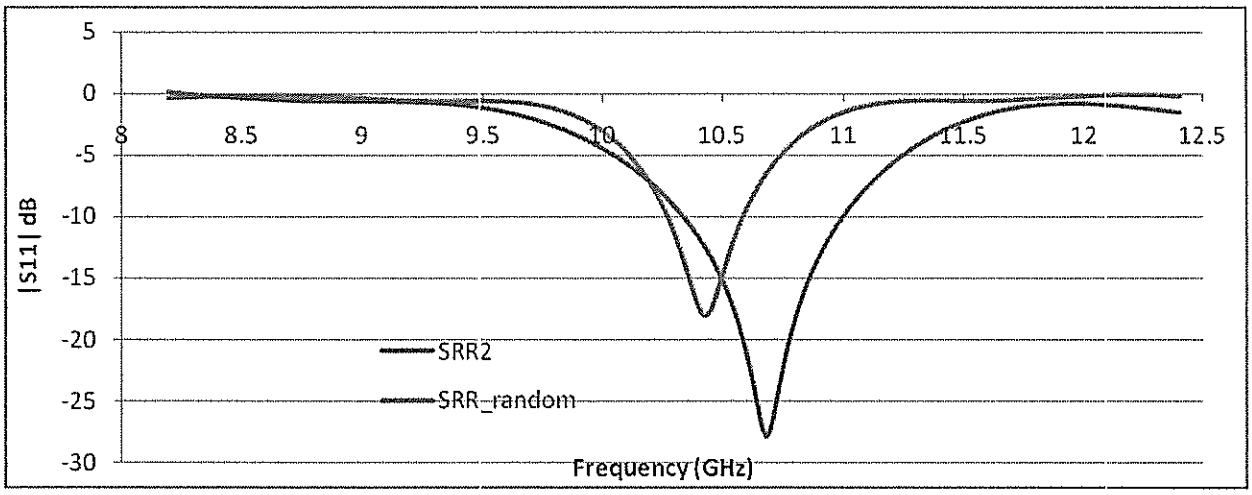

Figure 11 – Experimental result for SRR2 and SRR_{random} with metal backing. S_{21} is at the dynamic floor of the network analyzer and is a trivial result. Near 100% incident power is absorbed by these samples, 99.9% for SRR_2 and 98.3% for SRR_{random}.

4.6 Additional measurement

In order to compensate for a less densely packed sample in the case of planar SRR_{random}, measurements were performed by stacking samples in order to increase the density. The following measurement was made with metal backing. To add an additional sample to compare this result with, a Low Temperature Co-fired Ceramic (LTCC) SRR_2 sample was also measured. The results, shown below, verify that the density of a sample is crucial to the resonance strength as there are more oscillators to dissipate the incident power. As more layers are stacked, the

resonant frequency can be seen to shift. This is due to coupling between the layers of SRR samples. This occurs for stacked samples because the SRR's are deposited on several planes instead of a single plane as is the case with the standard samples. It is most likely this coupling which causes the dual resonance in the 3 layer stack of SRR_{random}.

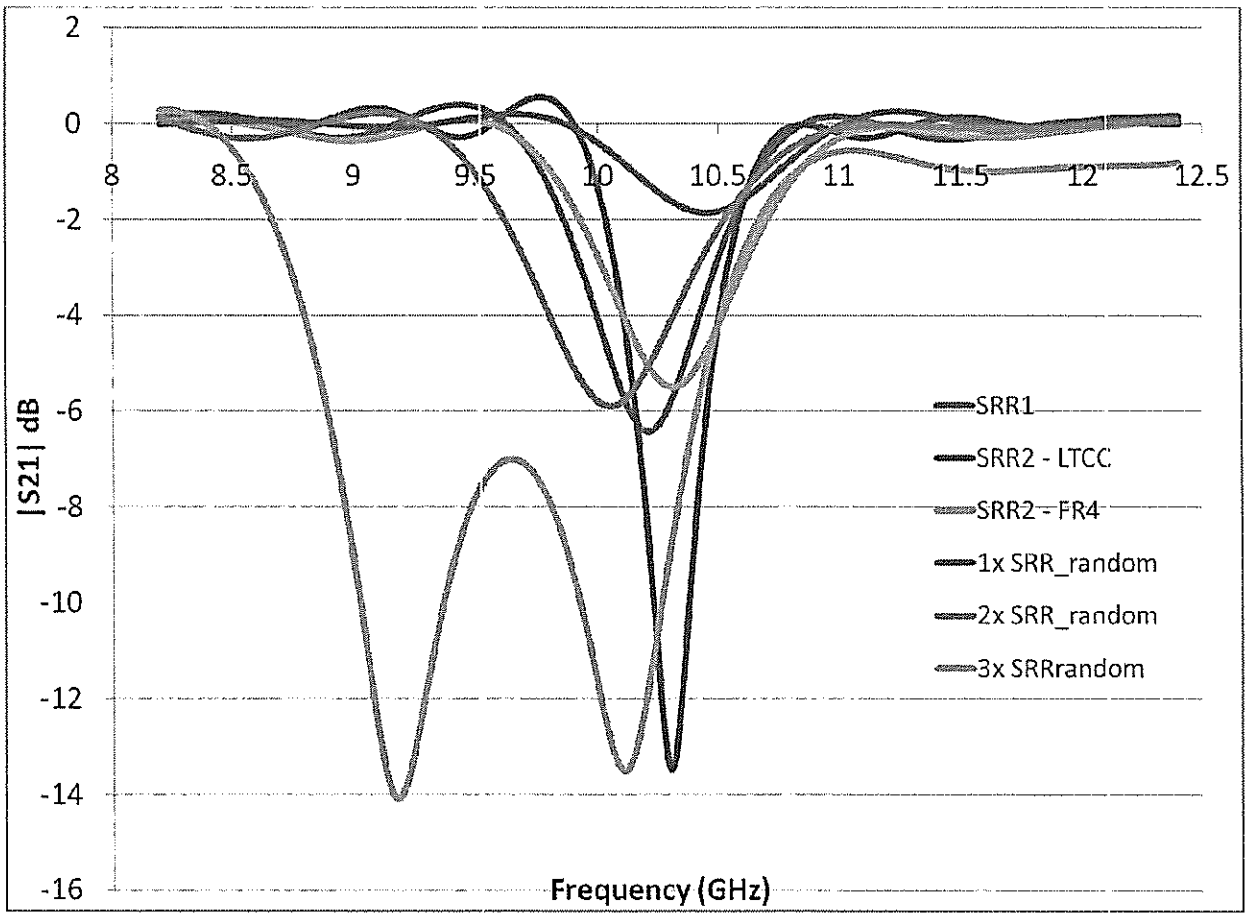

Figure 12 – measurement results for multilayer SRR_{random} as compared with standard SRR samples. The resonant frequency decreases with each additional layer due to coupling between layers of SRR.

5.0 Conclusions

Through experimentation, it is seen that a non-periodic arrangement of split ring resonators does not have any significant additional effect on resonance strength nor does offer a significant shift in resonant frequency. In the case of SRR_{random}, a difference in resonance strength can be attributed to less densely packed sample. The SRR_{random} samples consist of 500 SRR's over the same area as SRR_2 which has 900 SRR's; half the density. When the density of the sample is increased by stacking multiple layers, the resonant strength does indeed increase, while coupling between layers causes the resonant frequency to shift.

References

1. F. Bilotti, A. Toscano, L. Vegni, K. Aydin, K. B. Alici, E. Ozbay, "Equivalent-Circuit Models for Design of Metamaterials Based on Artificial Magnetic Inclusions,"IEEE Trans. MTT, vol. 55, no. 12, December 2007

2. V. V. Varadan, A. R. Tellakula, "Effective Properties of Split-Ring Resonator Metamaterials Using Measured Scattering Parameters: Effect of Gap Orientation," J. Appl. Phys. 100

3. F. Bilotti, A. Toscano, and L. Vegni, "Design of spiral and multiple split-ring resonators for the realization of miniaturized metamaterial samples," IEEE Trans. Antennas Propag., vol. 55, no. 8, August 2007

4. J. B. Pendry, A. J. Holden, D. J. Robbins, and W. J. Stewart, "Magnetism from conductors and enhanced nonlinear phenomena," IEEE Trans. Microw. Theory Tech., vol. 47, pp. 2075–2084, 1999.